ACS APPLIED MATERIALS & INTERFACES

Research Article

www.acsami.org

Cellular Interactions on Hierarchical Poly(ε-caprolactone) Nanowire Micropatterns

Ke Du[†,‡] and Zhihua Gan*[,†]

[†]The CAS Key Laboratory of Engineering Plastics, Institute of Chemistry, Chinese Academy of Sciences (CAS), Beijing 100190, China

[‡]The Graduate School of Chinese Academy of Sciences, Beijing 100049, China

ABSTRACT: A double template method to fabricate poly(ε-caprolactone) (PCL) hierarchical patterned nanowires with highly ordered nano- and microscaled topography was developed in this study. The topography of PCL film with a patterned nanowire surface can be easily and well controlled by changing the template and melting time of PCL film on the templates. The surface morphology, water contact angle, protein adsorption, and cell growth behavior on the PCL films with different surface structures were well studied. The results revealed that the PCL nanowire arrays and the hierarchical patterned nanowires showed higher capability of protein adsorption and better cell growth than the PCL film with smooth surface. Typically, the PCL surface with hierarchical nanowire patterns was most favorable for cell attachment and proliferation. The present study was innovative at fabrication of polymer substrates with hierarchical architecture of nanowires inside microscaled islands to gain insight into the cell response to this unique topography and to develop a new method of constructing the bionic surface for tissue engineering applications.

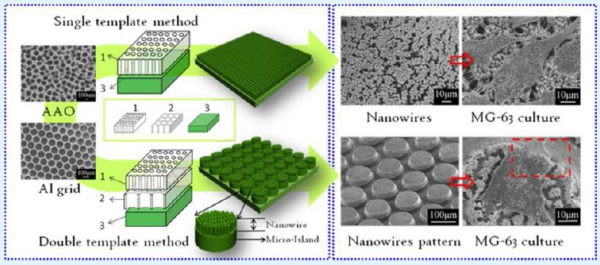

KEYWORDS: *double template, patterned nanowires, topography, cell adhesion, protein adsorption, poly(ε-caprolactone)*

1. INTRODUCTION

Recently, the construction of ordered hierarchical polymer nanostructures has drawn increasing attention.[1−3] Typically, polymeric nanowire or nanotube-based devices have great potential in tissue engineering application due to the advantage of unique surface properties such as nanoscale roughness, well-ordered alignment, large surface area, and spatially distinct surface topography from tall micropillar arrays. Since one of the key points of designing the artificial scaffolds is to mimic the physiochemical environment in native tissue by micro- and nanoscale physical manipulations,[4] the nanowire-based scaffold with high specific surface area and storage capacity would be an excellent candidate to satisfy the requirement. Many contributions have been made to develop the biological function of nanopillar structures. Fischer et al. found that the nanowires can served as a loading reservoir for therapeutic molecules with different sizes due to the significant increases in the loading capacity of nanowire coating compared with the smooth surface.[5] Besides, Yu et al. proposed poly(methacrylic acid) modified silicon nanowire arrays (SiNWAs) to be an ideal substrate for protein immobilization and separation because of the high surface area and enhanced local topographic interactions.[6]

Cells carry on their biological activities on the basis of good adhesion on the surrounding extracellular matrix substrates. In this case, the initial adhesion and subsequent biological behaviors are highly regulated by the local environment of chemistry and topography on mesoscale, microscale, and nanoscale sizes.[7−10] The nanopillar surface was reported to perform significantly higher cell adhesion compared to control groups without any nanoarchitecture.[11]

The template approach has been extensively developed to prepare different kinds of nanostructures.[12,13] Nanoporous aluminum oxide (AAO), which contains arrays of straight cylindrical nanopores with uniform size in length and diameter, has been widely used as an inorganic model matrix to fabricate inorganic/organic nanowires.[14] Given the fact that polymeric melts could infiltrate into the nanopores of the AAO templates by capillary action and the template can be easily removed by exposure to sodium hydroxide, it is also a convenient and inexpensive route to fabricate oriented nanowire arrays of biodegradable polymers without the use of organic solvents, pressure assistance, or custom instrumentation. Several attempts have been made to fabricate the well-defined nanowire alignment using biodegradable polymers with AAO as template, such as poly(ε-caprolactone) (PCL) nanowire arrays.[15] Grimm et al. fabricated the ordered arrays of aligned nanorods with diameter of 180 nm using poly(DL-lactide) (PDLLA). The cellular interactions of fibroblasts with PDLLA nanorod arrays show that the dense layers of locally aligned fibroblasts with excellent viability and likewise excellent morphological properties were obtained on the PDLLA nanorod arrays.[16] Also, the

Received: June 5, 2012
Accepted: August 8, 2012
Published: August 8, 2012

dx.doi.org/10.1021/am301013e | *ACS Appl. Mater. Interfaces* 2012, 4, 4643−4650

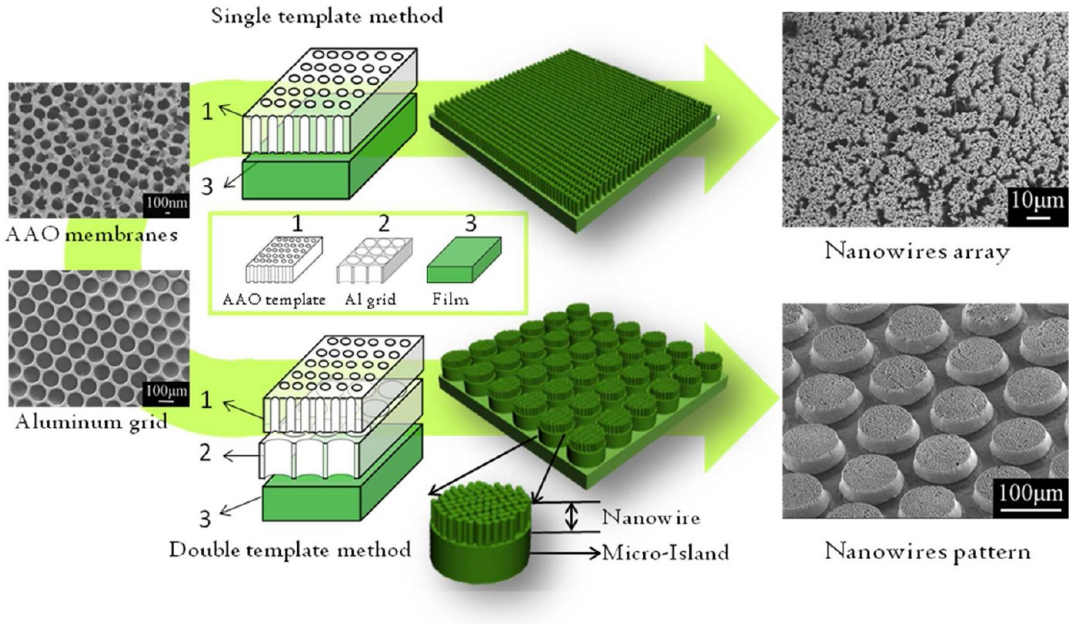

Figure 1. Schematic presentation of the fabrication process of a homogeneous PCL nanowire array by the single-template method and highly ordered hierarchical PCL nanowire patterns by the double template method.

cellular interactions of rat pheochromocytoma (PC12) and Mesenchymal stem cell (MSC) cell lines with PCL nanowire arrays were reported by Popat et al.[4,11] The two types of cell lines employed in the studies showed enhanced short-term biocompatibility and long-term bioactivity on nanowire surfaces as compared to the control surfaces.

Though pillar-array structures of biodegradable polymers can be generated by AAO-template techniques, how to control the surface hierarchical topography with different scale grades is seldom reported. Herein, a simple method to fabricate hierarchical PCL patterned nanowires with highly ordered nano- and microscaled topography was developed. We utilized the aluminum grid as the first template and mesoporous aluminum oxide membrane as the second template to generate a microscaled island with nanowire structure. By means of this double-template method, well-defined hierarchical patterned nanowires were successfully fabricated. The influences of patterned nano- and microstructures on the surface wettability and protein adsorption properties were evaluated. We also use a human osteosarcoma cell line (MG-63) to evaluate the cell response to the hierarchical patterned nanowire surfaces. The results revealed that the patterned surface with nano- and microscaled coexisting structure provide a more preferable environment for promoting cell adhesion and proliferation.

2. EXPERIMENTAL SECTION

2.1. Materials. Poly(ε-caprolactone) (PCL) (M_w = 65 000; M_n = 42 500) was purchased from Aldrich. AAO template (AnoporeTM) was purchased from Whatman. Aluminum grids were purchased from Beijing Xinxingbairui Co. Bovine serum albumin (BSA) and fibrinogen were purchased from Sigma. Human osteoblast-like cells (MG-63) were obtained from Cell Resource Centre (IBMS). Hoechst33342 and Phalloidin-TRITC were purchased from Sigma–Aldrich. Penicillin streptomycin was purchased from Solarbio, China. CCK-8 was purchased from Dojindo (Japan). Medium Dulbecco's modified Eagle medium (DMEM) and fetal bovine serum (FBS) were obtained from Hyclone. All other materials were commercially available and used as received unless otherwise mentioned. Other chemical reagents used in this work were all of analytical grade and purchased from Beijing Chemical Co. China.

2.2. Preparation of PCL Patterned Nanowires. Well-defined hierarchical nanowires were fabricated by means of the double-template method with AAO membranes and aluminum grid as templates. The preparation technique was illustrated in Figure 1. Typically, PCL was first cast into film with a thickness of 150 μm. The PCL film was then covered on the alumina grid and aluminum oxide membrane one by one and placed on a hot stage at 80 °C for 30 min in order to form the hierarchical pattern. After cool down to the room temperature, the combination of PCL film and two templates was put into 1 M NaOH solution and stirred for 60 min. The as-obtained PCL patterned nanowires were rinsed thoroughly with distilled water, freeze dried, and stored in a desiccator until further analysis.

2.3. Preparation of PCL Nanowire and Microisland Surfaces. Nanowires were fabricated via single template according to an established procedure.[4] In brief, PCL film was placed on the surface of AAO membrane at 80 °C for 5 min. After cool down to the room temperature, the AAO membranes were dissolved in 1 M NaOH for 60 min. The as-obtained PCL nanowires were then rinsed profusely with distilled water, dried under vacuum, and stored in a desiccator until further analysis. In the same way, the PCL microislands were fabricated following the above method, only using an Al grid instead of an AAO membrane.

2.4. Surface Characterization. The morphology of PCL film surface with nano- and microscaled structures was observed by field-emission scanning electron microscopy (JEOL JSM-6700F Japan) after being vacuum coated with gold. The static contact angle measurements of all samples were performed by the sessile drop method, using a Dataphysics OCA20 (optical contact angle measurement) device equipped with a Nikon Camera. The measurements were performed at room temperature with deionized water as probe liquid. The volume of each drop was 2 μL. Each contact angle reported here is an average from a set of at least five drops, and the contact angles were determined according to the direct optical images by a camera and calculated using image analysis software.

2.5. Protein Adsorption. Protein adsorption was performed by incubating the PCL films with different surface structures in phosphate buffered saline (PBS, 0.1M, pH = 7.4) containing 10 wt % BSA or fibrinogen. The disk-like specimens with dimensions of 10 mm in diameter and 150 μm in thickness were used. Specimens were then put into 24-well culture plates (one specimen for each well), and 1 mL of

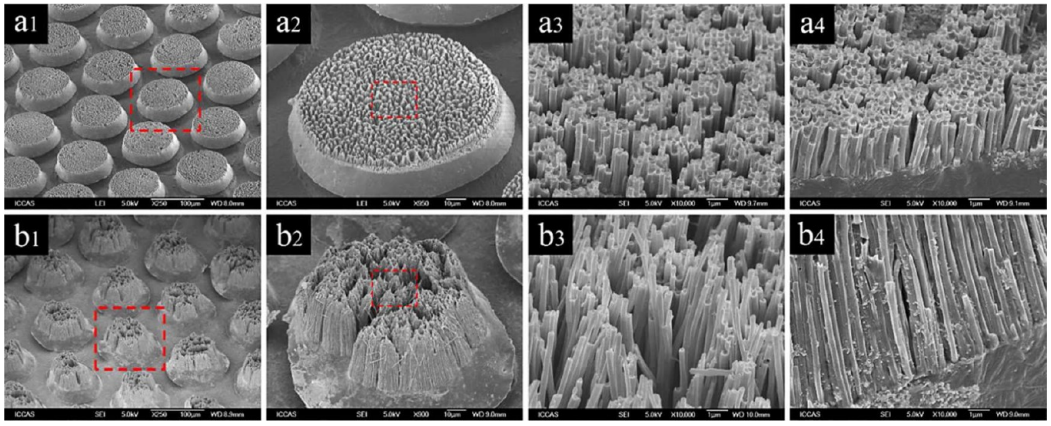

Figure 2. Typical SEM images of hierarchical PCL nanowire patterns prepared with different annealing times (a: 30 min, b: 120 min; a1 and b1: ×250; a2 and b2: single microisland unit, × 250; a3 and b3: top view of the nanowires, ×10 000; a4 and b4: side view of the microisland unit, ×10 000).

FBS/PBS solution was added into each well. After incubating at 37 °C for a given time, the concentration of the protein in the FBS/PBS solution was then quantified with a commercial BCA protein assay kit using bovine serum albumin (BSA) standards. The amount of absorbed proteins was determined by subtracting the amount of proteins left in the FBS/PBS solution after adsorption from the amount of proteins in the control FBS/PBS solution (without specimen) under the same incubation conditions.

2.6. Cell Growth. Human osteoblast-like MG-63 cells were cultured in Dulbecco's modified eagle medium, supplemented with 10% fetal bovine serum and 1% penicillin streptomycin. Cells were precultured in medium at 37 °C in a humid environment with 5% CO_2. After having passaged for three generations and reaching 80−85% density, the MG-63 were collected from the Petri dish and seeded onto the film samples. Prior to cell seeding, all the round films in a radius of 5 mm and thickness of 150 μm were sterilized in 75% ethanol for 3 h, followed with UV irradiation for 1 h, and then immersed in culture medium. The film samples were then placed into a 24-well plate, and the cells (250 μL suspensions) were seeded at a density of 5−6 × 10^4cells/mL. The cell-seeded samples were cultured at 37 °C in an incubator with 5% CO_2 atmosphere for 8 days. The culture medium was replaced every 2 days during the culture period.

Cell morphology was studied by scanning electron microscopy (SEM; JEOL JSM-6380LV). The cell/sample construct was fixed by 2.5% glutaraldehyde for 30 min and then dehydrated through a series of graded alcohols. After being lyophilized, the samples were fixed onto stubs and sputter coated with gold for SEM observation.

Cell morphologies were further observed by confocal laser scanning microscopy (CLSM) (OLYMPUS FV1000-IX81). The cell/sample construct was fixed by 2.5% glutaraldehyde for 30 min and then stained with Phalloidin−Tetramethyl rhodamine B isothiocyanate (Phalloidin-TRITC) for 60 min to label cell actin and followed by DNA staining with Hoechst33342 for 10 min. After staining, the cell/sample construct was rinsed with PBS for CLSM observation.

Cell adhesion and proliferation on the samples were quantitatively measured by cell counting kit-8 (CCK-8) with a microplate reader (MULTISKAN MK3, Thermo Electron Co.). The tested samples (UV-sterilized) were placed into the 96-well plate. A MG-63 human osteosarcoma cell suspension (100 μL) with a cell density of 5 × 10^4 cells/mL was seeded upon the samples. The cell-seeded samples were incubated at 37 °C in a humidified atmosphere (5% CO_2) for a period of up to 7 days, with the medium changed every 2 days. Cellular culture medium was aspirated before performing CCK-8 assays. CCK-8 (100 μL, 10%) in DMEM was added to each well and incubated with the cells at 37 °C for 2 h. All the cell culture medium containing the CCK-8 solution was transferred into a new 96 well plate and then measured at 450 nm wavelength by the microplate reader.

3. RESULT AND DISCUSSION

3.1. Fabrication of Hierarchical PCL Nanowire Arrays. The typical procedure for fabricating highly ordered hierarchical PCL nanowire patterns via a double-template technique is given in Figure 1. The aluminum grid, served as the first template, is characterized by regular circular arrays of parallel pores with sharp pore size distributions. The thickness of the grid is about 15 μm, and the aperture size can be chosen for 150, 100, and 65 μm. The purpose of this template is to generate the first microscaled island structure. Anodic aluminum oxide (AAO) templates were used as the second template to generate nanowire patterns on the top of island structure, giving rise to a secondary length scale. The commercially available AAO membranes, with a highly ordered hexagonal array of nanopores in alumina, have pore lengths of 60 μm and diameter of 200 nm or 100 nm. When PCL film was placed on the two layers of templates at 80 °C, the polymer melt penetrated the two templates in proper order. After infiltrating the first template and forming the microscaled island structure, the polymer melt proceeded to draw into the AAO membrane by wetting the surface of the pore walls.[17] The cylindrical nanopores of porous AAO template are gradually filled with polymer melts via capillary effect.[18] The flow rate of polymer melt in the cylindrical nanopores can be estimated by the following equation[19]

$$\frac{dz}{dt} = \frac{R\gamma\cos\theta}{4\eta z} \quad (1)$$

where t is annealing time; z is the height of the polymer melts drawn into the nanopore; R is the radius of nanopores; γ is the surface tension; η is the viscosity of polymer melts. As can be seen in eq 1, filling the cylindrical nanopores in the alumina membranes with polymer melts via the capillary action is mainly dependent on three controllable external factors: time, annealing temperature, and the pore diameter of the AAO template. By changing the three factors, the length and diameter of the nanowire could be well controlled. The nanopillar with ultrafine high aspect ratio is prone to cluster induced by lateral forces resulting from capillary menisci interaction.[20] In this respect, the homogeneous controlled arrays of PCL nanowires can be obtained by controlling the template reaction time to dominate the aspect ratio.

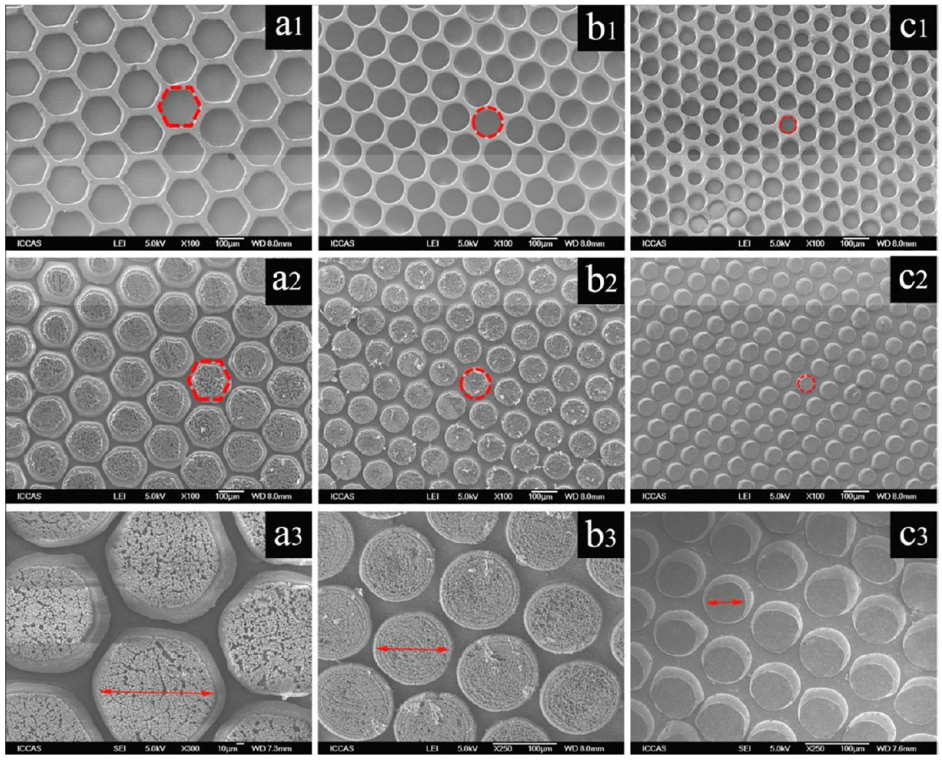

Figure 3. Typical SEM images of hierarchical PCL nanowire patterns prepared with aluminum grid of (a) 150 μm, (b) 100 μm, and (c) 65 μm in pore diameter (a1−c1 aluminum grid; a2−c2 as-obtained PCL nanowire pattern; a3−c3 magnified SEM images of a2−c2).

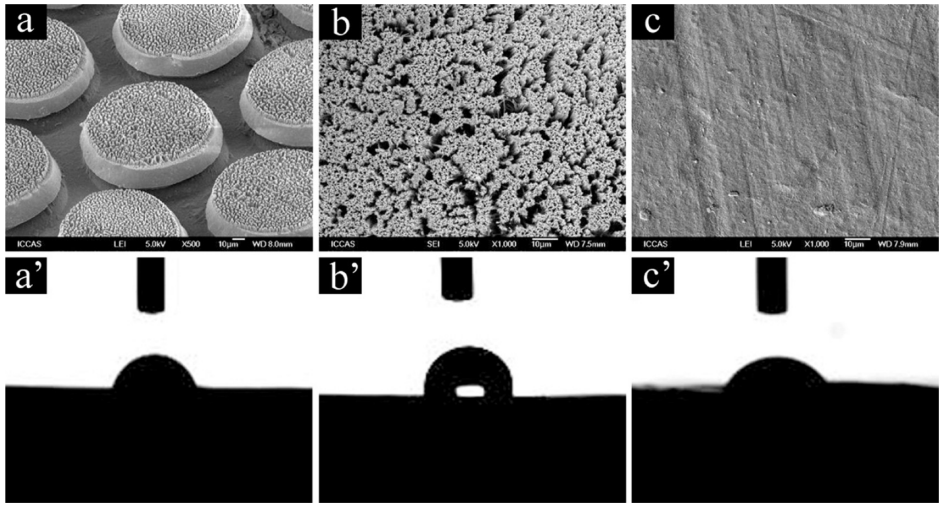

Figure 4. Typical SEM images of the systematically modified surfaces (a, PCL nanowire pattern; b, PCL nanowire; c, PCL film) and the corresponding initial water contact images.

Figure 2 shows the SEM morphology of hierarchical PCL nanowire patterns prepared with different template reaction time. Short template reaction time resulted in the formation of bare microisland structure. However, when the template reaction duration is long enough, the PCL melt was able to infiltrate the nanopores of AAO membrane via capillary action to form the nanowires in the island. As shown in Figure 2 (a3 and a4), the average length of the nanowires reached 2 μm with duration of 30 min. When the template reaction duration was further prolonged to 120 min, the corresponding average length of nanowires could reach about 20 μm (Figure 2 (b3,b4)).

To control the distribution region of the nanowires, the selection of the first template is essential. As shown in Figure 3, the area of the microscaled islands and the bridge spaces between adjacent islands could be controlled by choosing template with different pore size. Three templates with aperture of 150 μm (Figure 3 (a1−a3)), 100 μm (Figure 3 (b1−b3)) and 65 μm (Figure 3 (c1−c3)) were chosen as the first templates to generate different hierarchical PCL nanowire patterns. The Al grid with 150 μm in pore size can generate hexagonal shape islands with a larger diameter, while the Al grid with 65 μm in pore size creates smaller and denser microislands. Besides, it is noted that when the Al grid with 65 μm in pore size was used it failed to generate nanowires on the top of the microscaled island. Consequently, the morphology and roughness of the patterned nanowires with

controlled nano- and microscaled structures were able to be fabricated, which provides a variable microenvironment for cell seeding and growth.

Surface wettability is an essential factor in designing the scaffold. Figure 4 shows the typical SEM images of water droplet on the surface of PCL films with different micro- and nanoscaled structures. It is clear that the initial water contact angles on PCL nanowire arrays and hierarchical PCL nanowire patterns are relatively higher than on PCL films, which implies that the PCL surfaces become more hydrophobic after surface physical treatment for nano- and microstructures. The reason can be attributed to the nanoscale structure consisting of nanopillars and the tiny spaces between nanowires which served as an air-storage container. According to the modified Cassie's equation, surface hydrophobicity can be obviously intensified by increasing the proportion of water/air interfaces.[21] The nanowire construct allowed air to trap in the individual pillars and thus resulted in the increase of surface hydrophobicity.[22]

Figure 5 shows the water contact angle measurements on the systematically modified surfaces at 1 s and 10 s. At 1 s, the initial water contact angle for hierarchical PCL nanowire patterns, PCL nanowire arrays and PCL film is 81.1 ± 2.2°, 103.3 ± 3.5°, and 65.7 ± 4.2°, respectively. After 10 s, the surfaces of both the PCL nanowire arrays and hierarchical PCL nanowire patterns showed meaningful change in WCA. It was found that the average decline value of WCA after 10 s dwelling on the PCL nanowire arrays and hierarchical PCL nanowire pattern is 24.6° and 25.1°, respectively. However, the value is only 3.1° for PCL film with a smooth surface. The WCA change is owing to the hierarchical structure which ensures that there were adequate spaces for water droplets to permeate and spread on the PCL films with hierarchically nano- and microscaled structures.

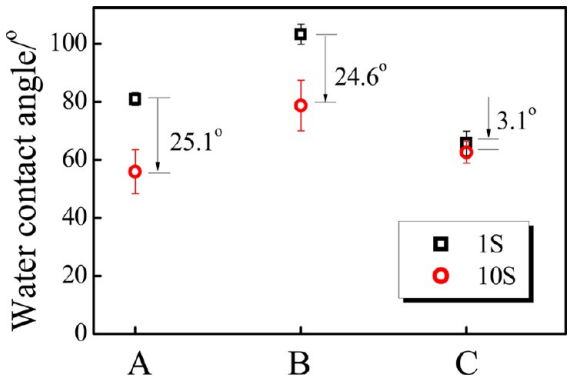

Figure 5. Water contact angle measurements of different droplets on the systematically modified surfaces at 1 and 10 s. (A) PCL nanowire pattern; (B) PCL nanowires; (C) PCL film.

Proteins at the cell−matrix interface play a vital role in mediating the adhesion behavior of cells on synthetic matrixes which lack cell binding ligands on the surface.[23] Thus, the protein absorption ability is considered to be one of the important factors for evaluating the biocompatibility and bioactivity of scaffolds. Figure 6 shows the protein absorption abilities of PCL nanowire pattern, PCL nanowire arrays, and PCL film. Two types of protein (fibrinogen and BSA) were employed as model proteins here, since albumin is considered to be the most abundant protein in blood plasma, while fibrinogen could help stop bleeding by helping blood clots to form. Therefore, both of the two type of proteins were critical protein models to evaluate the materials for biomedical application. On the basis of the results, it was found that the amount of proteins adsorbed on all substrates shows an obviously increasing tendency with an increase in the incubation time. For BSA adsorption, it is of great interest to note that the protein adhesion abilities of PCL nanowire arrays and the hierarchical PCL nanowire pattern are more than 3-fold higher than PCL films. This enhanced protein adhesion phenomenon may be ascribed to the increased surface area or complicated topography of substrates. It is a general trend that protein adsorption increases with increasing hydrophobicity of the surface,[6] so the improvement of the hydrophobicity caused by the nanoscaled structure may account for the reason. In addition, the increased surface area due to the complicated topography of nanowires could improve the loading capacity of protein. Evidently, the hierarchical PCL nanowire pattern and PCL nanowire arrays may be ideal substrates for protein immobilization due to their high surface area and enhanced local topographic interactions. It is found that the BSA absorption capacity of all the three surfaces is higher than that of fibrinogen, indicating a better selective absorption with BSA protein for PCL-based substrate compared to the fibrinogen protein. The mechanisms governing the interaction between protein and polymer could be polyelectrolyte absorption[24] and hydrophobic and ionic interactions, depending on the substrate and type of proteins involved.

In the present study, human osteosarcoma cell line (MG-63) was used to evaluate the ability of patterned nanowire surfaces for maintaining the cell adhesion and growth. Figure 7 shows the viability of cells incubated with various substrates evaluated

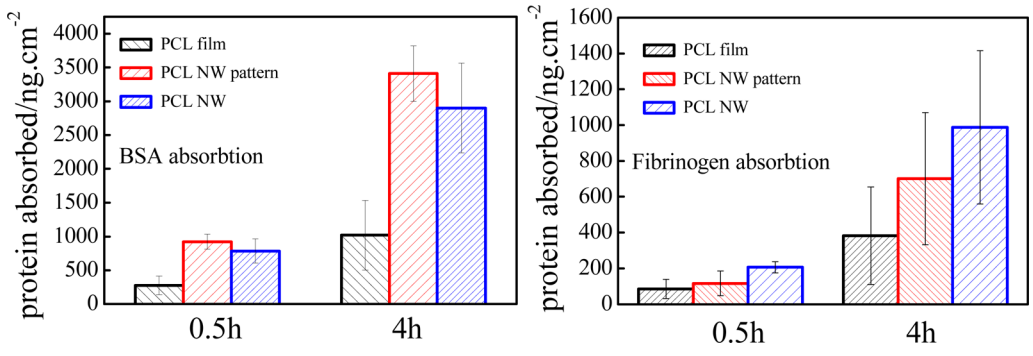

Figure 6. Protein absorption assays on PCL films with different hierarchical structures.

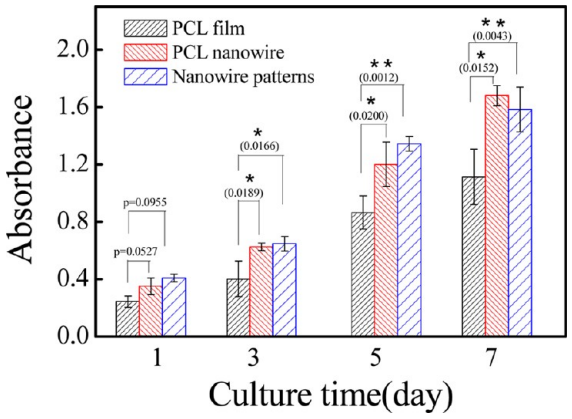

Figure 7. A comparison of the proliferation of MG63 cells on PCL films with different surface structures after 1, 3, 5, and 7 days of culture. (∗ indicates significance with $p < 0.05$, and ∗∗ indicates significance with $p < 0.01$, respectively. All data was analyzed using STATA software and was shown as means ± standard deviation. The significance of the obtained data was performed using ANOVA analysis of variance, and $p < 0.05$ was considered to indicate a statistically significant difference. The error bars denoted the standard deviation, and each experiment was repeated at least three times.)

by the CCK-8 assay.[25,26] Initial cell viability was different among three groups observed at day 1, showing 0.244 ± 0.038 for PCL film, 0.350 ± 0.059 for PCL nanowire arrays, and 0.409 ± 0.027 for hierarchical PCL nanowire patterns in optical density (OD) value. These results revealed that the coexistence of nano- and microscaled structures will provide a more preferable environment for cell seeding. Obviously, the same tendency was continued as the cell proliferation was observed at days 3, 5, and 7. Hierarchical PCL nanowire patterns demonstrated better cell compatibility on its surface, evidenced by the significant increase in OD value from 0.647 at day 3 to 1.584 at day 7, which indicated a remarkable cell proliferation behavior. However, the PCL film showed a relatively smaller amount of cell adhesion and proliferation rate at any given time point. Therefore, it can be concluded that all the PCL substrates were nontoxic and cell biocompatible, while the PCL film with nano- and microscaled structure on the surface were more suitable for cell activities.

In order to observe the cell adhesion status, MG-63 cells were incubated with a hierarchical PCL nanowire pattern and PCL nanowire arrays for 2 days. As a control, PCL film and PCL microscaled island substrate were also employed to examine the cell response. The results were shown in Figure 8. For PCL plat film (Figure 8 (a,a′)), MG-63 cells appeared to be more elongated and little pseudopodia were observed. However, for PCL nanowire surfaces (Figure 8 (b,b′)), MG-63 cells demonstrated polygonal shape and the size of polygonal cells was much larger than those on PCL films. Especially, the MG-63 cells had pronounced elongated filopodia from cell edges which closely touched with the nanoscaled pillar structure (Figure 8 (b′)). Such kind of fully extended filopodia plays an important role in the adhesion and spread of cells on substrates, indicating the improvement of nanowire structure for cell anchorage and growth.

For the PCL patterned nanowires, the nanoscaled structure in the microdomain was found to play a significant role in the cell growth. As shown in Figure 8 (c,c′), the MG-63 cells preferred to adhere on the nanowire surface of microscaled patterns. In addition, the MG-63 cells were totally wrapped

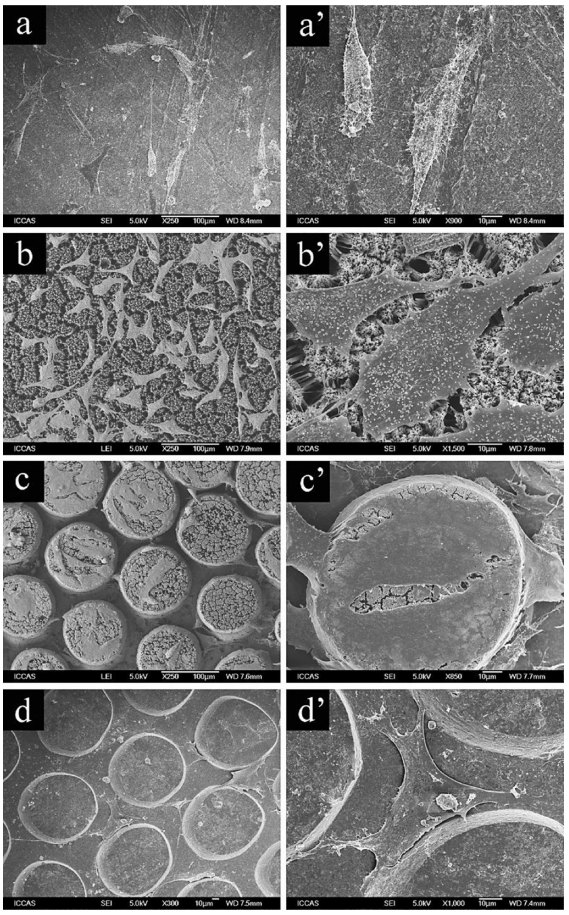

Figure 8. SEM images of MG-63 incubation with four kinds of substrates for 2 days. (a) flat PCL film; (b) PCL nanowire; (c) PCL patterned nanowires; (d) microscaled islands without nanowires.

around microscaled islands and spread along the microisland walls. However, for the control group without nanowires in the microscaled islands (Figure 8 (d,d′)), the MG-63 cells were mainly distributed in the interspace of isolated islands and only a few cells were observed on the top surface of the island.

Figure 9 showed the representative CLSM images of MG-63 cells after being seeded for 2 days on the hierarchical PCL patterned nanowires and the control group without nanowires in the microscaled islands. It is evident that cells were prone to adhere and spread on the nanowire surface of microscaled patterns (Figure 9 (a,b)), indicated by a high degree of cell aggregation within the circular island region. This result was consistent with SEM results. However, MG-63 cells distribute irregularly and independently on the control group without nanowires in the microscaled islands (Figure 9 (c,d)). Moreover, actin filaments of MG-63 cells on the nanowire surface of microscaled patterns were displayed as a network of long and well-defined stretched fibers, which reflected a full spreading of MG-63 cells on the nanowire section. Actin was reported to be of great importance in transmitting extracellular forces to the cells via integrins and played a crucial role in inducing signal transduction for cell function.[16] Thus, the CLSM results indicate that the cell function responded more rapidly on the nanoscaled topology surfaces.

The differences of cell distribution on PCL patterned nanowire surfaces and the control group without nanowires in the microscaled islands are undoubtedly attributed to the

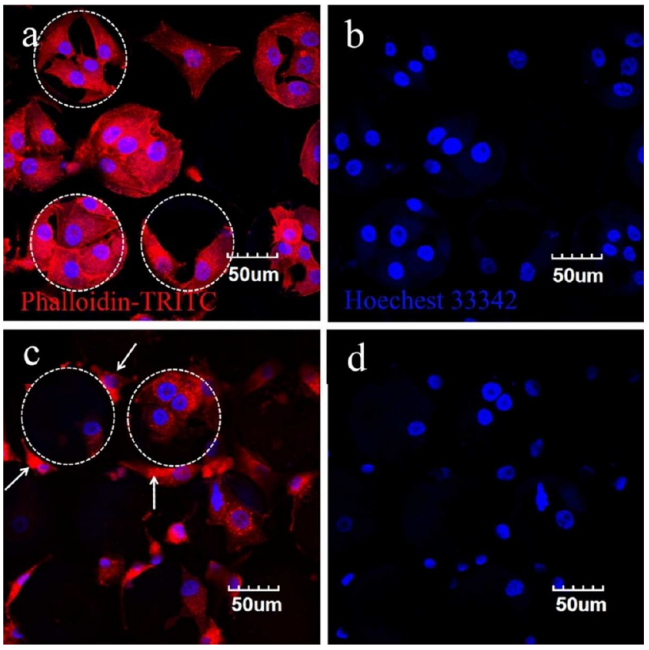

Figure 9. Confocal laser scanning microscopy (CLSM) images of MG-63 cells grown for 2 days on the PCL nanowire patterns (a and b) and PCL microscaled islands (c and d). The cells were fixated with glutaraldehyde and stained. The nuclei are blue (stained by Hoechest 33342), and the presence of actin filaments is indicated by the red color (stained by Phalloidin-TRITC). The circles of dashed lines indicate the microscaled islands.

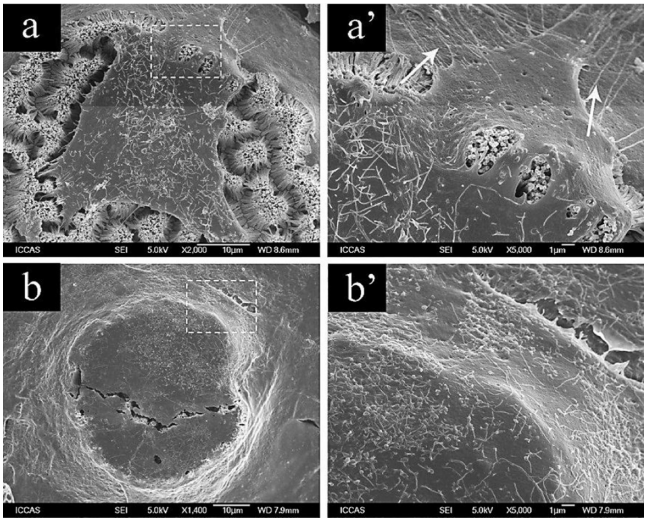

Figure 10. Comparative SEM images of MG-63 cells incubated with PCL nanowire patterns for 2 days (a and a′) and 6 days (b and b′). The images of a′ and b′ are the magnification of images of a and b, respectively.

presence of nanowire on the top of microscaled islands. It was reported that the nonflat and needlelike nanostructures stimulate cells to extend more filopodia to form focal adhesion points to substrate when cells first come into contact with the nanopillar arrays.[27] Our results here indicate that the cells seeded on nanowire surfaces had a rapid morphological response rather than on the smooth surfaces.

Cell−material interaction is a fundamental procedure for cell growth and survival and its quality directly determines subsequent cellular events.[28] At normal state, cells continuously extend and contract lamellipodia in all directions as if searching for a "sticky" site, then elongating in one direction before snapping back to a round morphology (which sometimes resulted in cell detachment) to begin the search process once again.[23] In this work, our results revealed that the nanopillar surface could provide a sufficient site for cellular lamellipodia to grasp, so the MG-63 cells preferred to adhere on the nanowire region rather than the flat surface. Except for the nanotopography, the other possible explanation for the pronounced cell affinity of the nanowire structure may be attributed to the enhanced protein storage and immobilization ability of the nanowire surfaces. As is well-known, once specific proteins or peptide sequences on the substrate are immobilized, cells can readily attach and proliferate.Undoubtedly, proteins play critical roles in mediating cell adhesion, spreading, and proliferating. Besides, our results revealed an interesting phenomenon that MG-63 cells showed a tendency of growth in three-dimensional forms in the case of hierarchical PCL patterned nanowires, which could be clearly seen in Figure 10.

Figure 10 shows the typical SEM images of cell morphology cultured on the hierarchical PCL nanowire pattern after 2 days and 6 days. It is clear that the MG-63 cells spread on the nanowires and changed their skeleton in order to grow along the walls of the microislands at an early stage (2 days culture in Figure 10 (a,a′)). After a culture duration of 6 days, the MG-63 cells fully covered the microscaled islands and contacted closely with the nanopillar on the top of islands (Figure 10 (b,b′)). The MG-63 cells integrated into a thick layer, and the single cell edge was invisible due to the proliferation.

Figure 11 shows the typical SEM images of cell morphology after incubation for 6 days on the microislands without a nanowire structure. It was found that MG-63 cells adhering on the smooth surface of islands cannot cling to the lateral part of the islands. Instead, the MG-63 cell growth was stopped by the interspace of islands, resulting in the poor adhesion of cells on the substrate. The different cell response on the substrates with different topography implied that the hierarchical patterned nanowires possessed a better cellular biocompatibility. Strongly supported by the reports that the topographical pattern affects the cell growth behavior, including triggering changes in cell shape and the subsequently induced alterations in the function and viability of the cells,[28−30] our results provide a very simple double template method to construct the polymer substrates with nanoscaled and microscaled structures for promoting cell growth behavior.

Figure 12 illustrated the schematic representation of the mechanism of the cell growth process on the microislands without a nanowire surface (a) and the three-dimensional growth processes of MG-63 cells on the hierarchical PCL patterned nanowires (b). On the basis of the CLSM and SEM results, it can be concluded that the MG-63 cells strongly prefer to adhere and spread on the nanowire surface of microscaled patterns. With the help of the lateral walls of nanowires in the islands, the MG-63 cells could wrap the whole microisland after further proliferation, exhibiting cell growth in 3-dimensional ways. However, for the microislands without the nanowire surface, the MG-63 cells distributed irregularly on the island top and in the interspace of islands, which were attributed to the lack of a "sticky" site on the smooth surface. Such kind of surface results in the cell growth in a plane form.

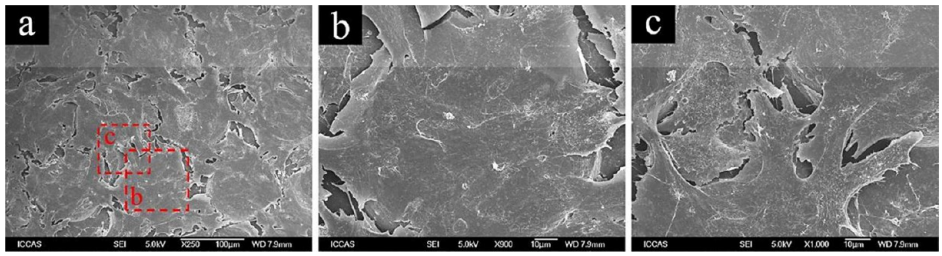

Figure 11. Typical SEM images of MG-63 cells incubated with PCL microislands for 6 days.

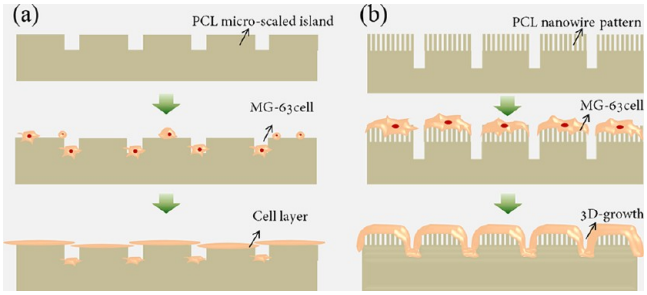

Figure 12. Schematic pictures of MG-63 cultured on microislands (a) and nanowire patterns (b).

4. CONCLUSION

A double-template method was developed here to fabricate PCL films with hierarchical patterned nanowires on the surface. The PCL nanowire arrays and the hierarchical patterned nanowire surface induced the higher capacity of protein absorption compared to the PCL film with a smooth surface. Surfaces with nanowire topography provided pronounced cell affinity compared with a smooth surface. Besides, it is interesting to find that cells responded to the patterned nanowires uniquely, by means of growing in a 3-dimensional form. This solvent-free and convenient double-template method for fabricating polymeric patterned nanowires provides an efficient approach for the construction of artificial scaffolds with nanoscaled and microscaled structures for tissue engineering application.

AUTHOR INFORMATION

Corresponding Author

*Tel/Fax: +86-10-62529194. E-mail: zhgan@iccas.ac.cn.

Notes

The authors declare no competing financial interest.

ACKNOWLEDGMENTS

This work was supported by the National Natural Science Foundation of China (Grant No. 51025314), the MOST 973 Project (2012CB933801), and the "Strategic Priority Research Program" of the Chinese Academy of Sciences (Grant no XDA01030301).

REFERENCES

(1) Cheng, Z.; Gao, J.; Jiang, L. *Langmuir* **2010**, *26*, 8233−8238.
(2) Karagiovanaki, S.; Koutsioubas, A.; Spiliopoulos, N.; Anastassopoulos, D. L.; Vradis, A. A.; Toprakcioglu, C.; Siokou, A. E. *J. Polym. Sci., Part B: Polym. Phys.* **2010**, *48*, 1676−1682.
(3) Liu, R. L.; Han, J.; Chen, X. J.; Lei, S. H.; Liu, H. Q. *Acta Polym. Sin.* **2012**, *3*, 291−298.
(4) Porter, J. R.; Henson, A.; Popat, K. C. *Biomaterials* **2009**, *30*, 780−788.
(5) Fischer, K. E.; Jayagopal, A.; Nagaraj, G.; Danies, R. H.; Li, E. M.; Silvestrini, M. T.; Desai, T. A. *Nano Lett.* **2011**, *11*, 1076−1081.
(6) Yu, Q. A.; Chen, H.; Zhang, Y. X.; Yuan, L.; Zhao, T. L.; Li, X.; Wang, H. W. *Langmuir* **2010**, *26*, 17812−17815.
(7) Lai, M.; Cai, K. Y.; Zhao, L.; Chen, X. Y.; Hou, Y. H.; Yang, Z. X. *Biomacromolecules* **2011**, *12*, 1097−1105.
(8) Ho, Q.-P.; Wang, S.-L.; Wang, M.-J. *ACS Appl. Mater. Interfaces* **2011**, *3*, 4496−4503.
(9) Tian, Y.; Wang, Y.; Zhou, C.; Zeng, Q.; Tan, G. *Acta Polym. Sin.* **2010**, *10*, 1170−1174.
(10) Xua, Y.; Zhang, D.; Wang, Z.; Gao, Z.; Zhang, P.; Chen, X. *Chin. J. Polym. Sci.* **2011**, *29*, 215−224.
(11) Bechara, S. L.; Judson, A.; Popat, K. C. *Biomaterials* **2010**, *31*, 3492−3501.
(12) Lazzara, T. D.; Kliesch, T.-T.; Janshoff, A.; Steinem, C. *ACS Appl. Mater. Interfaces* **2011**, *3*, 1068−1076.
(13) Haberkorn, N.; Weber, S. A. L.; Berger, R.; Theato, P. *ACS ACS Appl. Mater. Interfaces* **2010**, *2*, 1573−1580.
(14) Duran, H.; Steinhart, M.; Butt, H. J.; Floudas, G. *Nano Lett.* **2011**, *11*, 1671−1675.
(15) Tao, S. L.; Desai, T. A. *Nano Lett.* **2007**, *7*, 1463−1468.
(16) Grimm, S.; Martin, J.; Rodriguez, G.; Fernandez-Gutierrez, M.; Mathwig, K.; Wehrspohn, R. B.; Gosele, U.; San Roman, J.; Mijangos, C.; Steinhart, M. *J. Mater. Chem.* **2010**, *20*, 3171−3177.
(17) Chen, J. T.; Chen, D.; Russell, T. P. *Langmuir* **2009**, *25*, 4331−4335.
(18) Zhang, M. F.; Dobriyal, P.; Chen, J. T.; Russell, T. P.; Olmo, J.; Merry, A. *Nano Lett.* **2006**, *6*, 1075−1079.
(19) Kim, E. X., Y. N.; Whitesides, G. M. *Nature* **1995**, *376*, 581−584.
(20) Chandra, D.; Yang, S. *Acc. Chem. Res.* **2010**, *43*, 1080−1091.
(21) Feng, L.; Li, S. H.; Li, H. J.; Zhai, J.; Song, Y. L.; Jiang, L.; Zhu, D. B. *Angew. Chem., Int. Ed.* **2002**, *41*, 1221−1223.
(22) Jin, M. H.; Feng, X. J.; Feng, L.; Sun, T. L.; Zhai, J.; Li, T. J.; Jiang, L. *Adv. Mater.* **2005**, *17*, 1977−1981.
(23) Ayala, R.; Zhang, C.; Yang, D.; Hwang, Y.; Aung, A.; Shroff, S. S.; Arce, F. T.; Lal, R.; Arya, G.; Varghese, S. *Biomaterials* **2011**, *32*, 3700−3711.
(24) Richert, L.; Boulmedais, F.; Lavalle, P.; Mutterer, J.; Ferreux, E.; Decher, G.; Schaaf, P.; Voegel, J. C.; Picart, C. *Biomacromolecules* **2004**, *5*, 284−294.
(25) Ou, W. F.; Qiu, H. D.; Chen, Z. F.; Xu, K. T. *Biomaterials* **2011**, *32*, 3178−3188.
(26) Kim, D.; Kim, S.; Jo, S.; Woo, J.; Noh, I. *Macromol. Res.* **2011**, *19*, 573−581.
(27) Qi, S. J.; Yi, C. Q.; Ji, S. L.; Fong, C. C.; Yang, M. S. *ACS Appl. Mater. Interfaces* **2009**, *1*, 30−34.
(28) Matschegewski, C.; Staehlke, S.; Loeffler, R.; Lange, R.; Chai, F.; Kern, D. P.; Beck, U.; Nebe, B. J. *Biomaterials* **2010**, *31*, 5729−5740.
(29) Davidson, P. M.; Ozcelik, H.; Hasirci, V.; Reiter, G.; Anselme, K. *Adv. Mater.* **2009**, *21*, 3586−3590.
(30) Nebe, B.; Luthen, F.; Lange, R.; Becker, P.; Beck, U.; Rychly, J. *Mater. Sci. Eng., C* **2004**, *24*, 619−624.